Research Article

Semen extracellular vesicles mediate vertical transmission of subgroup J avian leukosis virus

Liqin Liao [a,b,e,1], Weiguo Chen [a,b,e,f,1], Xiangyu Zhang [a,e], Huanmin Zhang [c], Aijun Li [d], Yiming Yan [a,b,e], Zi Xie [a,b,e], Hongxing Li [a,b,e], Wencheng Lin [a,b,e,f], Jingyun Ma [a,b,e,f], Xinheng Zhang [a,b,e,*], Qingmei Xie [a,b,e,f,*]

[a] Heyuan Branch, Guangdong Provincial Laboratory of Lingnan Modern Agricultural Science and Technology, College of Animal Science, South China Agricultural University, Guangzhou, 510642, China
[b] Guangdong Provincial Key Lab of Agro Animal Genomics and Molecular Breeding, Guangzhou, 510642, China
[c] USDA, Agriculture Research Service, Avian Disease and Oncology Laboratory, East Lansing, MI, 48823, USA
[d] College of Science and Engineering, Jinan University, Guangzhou, 510632, China
[e] Key Laboratory of Animal Health Aquaculture and Environmental Control, Guangdong, Guangzhou, 510642, China
[f] Guangdong Engineering Research Center for Vector Vaccine of Animal Virus, Guangzhou, 510642, China

ARTICLE INFO

ABSTRACT

Subgroup J avian leukosis virus (ALV-J) is a highly oncogenic retrovirus that has been devastating the global poultry industry since the late 1990s. The major infection model of ALV-J is vertical transmission, which is responsible for the congenital infection of progeny from generation to generation. Increasing evidence has suggested that extracellular vesicles (EVs) derived from virus-infected cells or biological fluids have been thought to be vehicles of transmission for viruses. However, the role of EVs in infection and transmission of ALV-J remains obscure. In the present study, semen extracellular vesicles (SE) were isolated and purified from ALV-J-infected rooster seminal plasma (SE-ALV-J), which was shown to contain ALV-J genomic RNA and partial viral proteins, as determined by RNA sequencing, reverse transcription-quantitative PCR and Western blotting. Furthermore, SE-ALV-J was proved to be able to transmit ALV-J infection to host cells and establish productive infection. More importantly, artificial insemination experiments showed that SE-ALV-J transmitted ALV-J infection to SPF hens, and subsequently mediated vertical transmission of ALV-J from the SPF hens to the progeny chicks. Taken together, the results of the present study suggested that ALV-J utilized host semen extracellular vesicles as a novel means for vertical transmission, enhancing our understanding on mechanisms underlying ALV-J transmission.

1. Introduction

Subgroup J avian leukosis virus (ALV-J) is a positive sense, single-stranded RNA virus, which belongs to the *Alpharetrovirus* genus of family *Retroviridae* (Neoplastic Diseases, 2013). ALV-J genome is 7.6 kb in length and mainly consists of *gag, pol,* and *env* genes, which encode Gag (including capsid protein p27), reverse transcriptase as well as integrase, and envelope glycoproteins consisting of protein gp85 and gp37, respectively (Payne et al., 1993; Venugopal et al., 1997; Bai et al., 1998). Since its discovery in the United Kingdom (Payne et al., 1991), ALV-J has been in the news media spotlight due to its global spread and devastating effects on poultry flocks in the world (FadlyandSmith, 1999; Landman et al., 2002; Li et al., 2020). Indeed, ALV-J infection remains pervasive throughout China and in other Asian countries (F. Meng et al., 2018; F. Meng et al., 2018; P Wang et al., 2018; Wang et al., 2020). Furthermore, the epidemic strains of ALV-J are not only capable to induce hemangiomas, myelocytomatosis and visceral neoplasms, but also to cause poor production performance and severe immunosuppression (Payne and Nair, 2012; Malhotra et al., 2015; Zhou et al., 2019). These evidences indicate that ALV-J may have been responsible for the tremendously economic losses within worldwide poultry industry (Wang et al., 2012; Shen et al., 2014).

* Corresponding authors.
E-mail addresses: xhzhang@scau.edu.cn (X. Zhang), qmx@scau.edu.cn (Q. Xie).
[1] Contributed equally to this work.

ALV-J can be readily transmitted vertically from hen to chicks via fertile eggs or horizontally from bird to bird by early contact (Rubin et al., 1962). Notably, vertical transmission of ALV-J is the major route of ALV-J infection and is more deleterious than horizontal route due to higher efficiency of transmission from eggs to progenies and higher efficiency of virus shedding. (Lin et al., 2013). Vertical transmission of ALV-J may occur through the venereal route resulted from mating of infected roosters and healthy hens (Smith and Fadly, 1994), which implies that ALV-J-infected roosters play a pivotal role in transmission of ALV-J and may be responsible for the congenital infection of chicks during reproduction from one generation to the next. Once the breeding flocks, particularly breeder roosters, are infected by ALV-J, it is reasonably assumed that a large number of commercial chickens would be infected by ALV-J as a result of vertical transmission. Therefore, an improved understanding of the mechanisms underlying vertical transmission of ALV-J is required to enable the development of novel therapies for control and elimination of the ALV-J infection.

The primary vector for vertical transmission of ALV-J is semen, a complex bodily fluid mainly composed of spermatozoa cells and seminal plasma (Dhama et al., 2014). In addition to the soluble constituents, a variety of semen extracellular vesicles (SE) are contained in the plasma (Vojtech et al., 2014; Welch et al., 2017). Extracellular vesicles (EVs), including SE, are double membraned vesicles derived from multivesicular bodies during the maturation of endosomes (Thery et al., 2002). Extracellular vesicles have been shown to contain a variety of biological materials, including proteins, lipids, and genetic material such as DNA, RNA and microRNA, which deliver their cargo to recipient cells, reportedly mediating intercellular communications and thus participating in various biological and pathological processes (Kalluri and LeBleu, 2020; Kumar et al., 2020). Over the past decade, a growing body of literature has shown that EVs play pivotal roles in viral pathogenesis and serve as vector for the transmission of a variety of viruses (Chahar et al., 2015; Urbanelli et al., 2019). For instance, EVs released from porcine reproductive and respiratory syndrome virus (PRRSV)-infected cells contain PRRSV RNA and proteins, which can mediate the transmission of PRRSV in both susceptible and non-susceptible naive cells (T Wang et al., 2018). EVs have also been shown to play dual roles in mediating the transmission of hepatitis A Virus (HAV) and hepatitis C Virus (HCV), thereby avoiding immune surveillance (Longatti, 2015). Intriguingly, several studies have shown that EVs serve as a novel mode of flavivirus transmission from arthropod to human cells (Vora et al., 2018; Zhou et al., 2018). Langat virus (LGTV)-infected tick cell-derived exosomes have been shown to contain infectious virus RNA and protein, which facilitate transmission of LGTV from tick to vertebrate host cells (Zhou et al., 2018). Dengue virus (DENV)-infected mosquito cell-derived exosomes contain infectious DENV RNA and proteins, which can serve as a means for DENV transmission from mosquito to mammalian cells (Vora et al., 2018). These studies highlighted the crucial role of EVs in viral life cycle. On the other hand, some viruses are reportedly evolved in hijacking cellular EVs pathways, such that to mediate viral infection and transmission (Urbanelli et al., 2019). One earlier study reported that ALV-J infection can promote the production of exosomes, and partial viral proteins were observed in ALV-J-infected DF-1 cell-derived exosomes (Wang et al., 2017), but the roles of EVs in ALV-J infection and transmission still largely need to be elucidated.

In this study, we aimed to understand the composition and functionality of extracellular vesicles from ALV-J-infected rooster seminal plasma (SE-ALV-J) in relation to ALV-J transmission and infection in chicken.

2. Materials and methods

2.1. Cell culture and viruses

Chicken embryo fibroblasts (CEFs) were prepared from 10-day-old Specific Pathogen Free (SPF) chicken embryos, which were obtained from Guangdong Wen's DaHuaNong Biotechnology Co., Ltd., as described previously (Federspiel and Hughes, 1997). CEFs and DF-1 cells (immortalized chicken embryo fibroblast cells) were cultured in DMEM (Thermo Fisher Scientific, Inc., USA) supplemented with 10% exosome-depleted FBS (System Biosciences, Inc.) and 1% penicillin-streptomycin at 37 °C with 5% CO_2. The ALV-J strain GD1109 (GenBank: accession no. JX254901.1) used throughout this study was associated with hemangioma and stored in our lab following propagation and titration in DF-1 cells.

2.2. Animal challenge experiments

A total of 15 one-day-old SPF male chicks were inoculated with 0.3 mL 1×10^5/mL $TCID_{50}$ of ALV-J strain GD1109 virus stock per chick intra-abdominally and inoculated once again when they were 5 days old. Anti-coagulated blood samples were collected from all the inoculated SPF male chickens every 4 weeks starting from the 4th week until the 24th week post-infection, and tested for ALV-J infection status by viral isolation as previously described (Fanfeng Meng et al., 2018). Another 15 one-day-old SPF male chicks and 30 one-day-old SPF female chicks were not infected and used as the healthy chick controls. All SPF White Leghorn chicks were purchased from Guangdong Wen's DaHuaNong Biotechnology Co., Ltd. and were raised in negative-pressure-filtered air isolators under quarantined conditions. All experimental protocols were approved by the Animal Ethics Committee at the South China Agricultural University (approval ID: SYXK-2019-0136).

2.3. Isolation and purification of semen EVs and free ALV-J

Semen samples were collected from experimentally ALV-J infected SPF White Leghorn roosters (n = 15) and healthy SPF White Leghorn roosters (n = 15), respectively. ALV-J-infected and uninfected rooster semen samples were pooled with every 5 roosters, respectively, and stored at −80 °C. The procedure for isolation and purification of SE-ALV-J and SE from mock-infected rooster semen samples (SE-Mock), as well as free ALV-J particles was as described previously (Bukong et al., 2014) with minor modifications. Briefly, ALV-J-infected and mock-infected rooster semen samples were thawed on ice and centrifuged ($300 \times g$, 10 min, 4 °C; $2,400 \times g$, 10 min, 4 °C; $10,000 \times g$, 30 min, 4 °C) to remove cellular debris. The seminal plasma was filtered through a 0.22-μm PVDF (EMD Millipore) and subsequently mixed with Exo-Quick reagent (System Biosciences, Inc., USA) at a ratio of 4:1 (seminal plasma: Exo-Quick), and incubated at 4 °C overnight according to the manufacturer's protocol. The mixture was then centrifuged at $1,500 \times g$ for 30 min at 4 °C to remove the supernatant. The resulting SE-ALV-J, free ALV-J and SE-Mock pellets were resuspended in PBS in 1/5 of the original volume of semen. Then, the SE-ALV-J, ALV-J and SE-Mock pellets were further purified using Exosome-human CD63 Isolation kit CD63-labeled-Dynabeads (Invitrogen; Thermo Fisher Scientific, Inc., USA) according to the manufacturer's protocol. After the isolation, SE-ALV-Js (the pellet) were separated from ALV-J virion (the supernatant). And among SE-ALV-J, SE-Mock and free ALV-J were used for downstream experiments. Finally, SE-ALV-J and SE-Mock were eluted from the Dyna-beads with 100 mmol/L ice-cold Glycine-HCl (pH 3.0) and neutralized to pH 7.4 using 1 mol/L Tris-HCl buffer (pH 8.5).

2.4. Electron microscopy and immunogold labeling

The purified SE-ALV-J, and purified ALV-J free particles were resuspended in PBS and then spotted onto Formvar-coated 400-mesh copper grids. Subsequently, the adsorbed SE-ALV-J, SE-Mock or virions were fixed in 4% paraformaldehyde at room temperature for 30 min. Excess liquid was removed using filter paper. The grids were negatively stained with uranyl acetate for 1 min and then observed using a transmission electron microscope (TEM; Talos F200S; Thermo Fisher Scientific, Inc., USA). For immunogold labeling, the SE-ALV-J or viral suspensions were deposited on Formvar-coated nickel grids and fixed with 4% para-formaldehyde for 10 min. After washing with PBS, the grids were blocked

with PBS containing 5% BSA for 30 min and incubated with primary antibody against CD63 (System Biosciences, Inc., USA) and gp85 (made in our laboratory), and then with 10-nm colloidal gold-conjugated secondary antibody (goat anti-rabbit IgG). Finally, the grids were washed five times with blocking buffer, rinsed in deionized water, and then negatively stained and visualized as indicated above.

2.5. Nanoparticle tracking analysis (NTA)

NTA was performed using a Nano-sight LM-10 instrument (Nano-Sight) according to the manufacturer's protocol. For each sample of SE-ALV-J and SE-Mock, NTA was performed for 1 min and measured three times. Size distributions and concentrations of each sample were obtained by analyzing 1 min videos of data collection using the NTA software (version 2.3). The results represent the mean $\pm$ standard deviation of SE-ALV-J and SE-Mock isolations.

2.6. RNA sequencing analysis

To exclude the contamination of RNA, the EVs were firstly treated with RNase to eliminate non-vesicular RNA. Total RNA was isolated from SE-ALV-J samples and SE-Mock samples using TRIzol® reagent (Thermo Fisher Scientific, Inc., USA) according to the manufacturer's protocol. The RNA samples from SE-ALV-J or SE-Mock were pooled (respectively) in equal amounts, and total RNA yield was determined using electrophoresis (Agilent Bioanalyzer 2100; Agilent Technologies, Inc., USA). The resulting RNAs from SE-ALV-J and SE-Mock samples were used to prepare the RNA sequencing library as previously described (Zhang et al., 2016). RNA sequencing was performed on an Illumina NextSeq 500 platform (Illumina, Inc.). The raw FASTQ files for each sample from the RNA-Seq were trimmed three times using Cutadapt software (Kechin et al., 2017). The trimmed reads were mapped to the Gallus gallus reference genome (galGal6), ALV-J strain GD1109 genomic sequences (GenBank accession no. JX254901.1), as well as its *gag*, *pol* and *env* coding region sequences (CDS) using Bowtie2 version 2.1.0 (Langmead and Salzberg, 2012).

2.7. SE labeling and uptake

The SE-ALV-J or SE-Mock were labeled with the red dye DiI (1,1′-Dioctadecyl-3,3,3′,3′-tetramethylindocarbocyanine perchlorate; Sigma-Aldrich; Merck KGaA, USA) according to the manufacturer's protocol. Briefly, DiI was diluted with PBS to a working concentration of 5 μmol/L, and added to SE-ALV-J-PBS or SE-Mock-PBS suspensions (v/v, 1:5). The dye solution and the SE-ALV-J-PBS or SE-Mock-PBS suspensions were mixed and incubated for 20 min. The labeled SE-ALV-J or SE-Mock were centrifuged and washed to remove the excess dye. DF-1 cells (2×10^4) were seeded in a Laser confocal petri dish and cultured overnight in DMEM with 10% FBS. DiI labeled SE-ALV-J or SE-Mock (25 mg/mL) were added to 60–70% confluent DF-1 cells in 5% CO_2 at 37 °C for 2 h. The cells were washed three times with PBS and labeled using a green fluorescent DiO (3,3′-Dioctadecyloxacarbocyanine Perchlorate; Sigma-Aldrich; Merck KGaA, USA) to stain the plasma membranes of the cells. The cells were fixed with 4% paraformaldehyde, permeabilized, blocked in 5% BSA solution, and subsequently incubated with an anti-gp85 antibody (made in our laboratory), followed by immunofluorescence staining with Alexa Fluor 594-conjugated anti-mouse IgG or Alexa Fluor 488-conjugated anti-mouse IgG secondary antibody (Thermo Fisher Scientific, Inc., USA). The cell nuclei were stained with DAPI. Imaging was performed using a confocal laser-scanning microscope (Leica X, Leica Microsystems, Inc., Germany) to detect the uptake of SE by DF-1 cells for 2 h and 4 h.

2.8. SE-ALV-J infection assays in vitro

RNase (sigma) was added to purified EVs and incubation for 1 h at 37 °C before infection. For Fifty-percent tissue culture infective dose

($TCID_{50}$) assays, purified ALV-J free particles or SE-ALV-J (diluted from 10^{-1} to 10^{-8} with DMEM) were added into 96-well plate (seeded with 5×10^4 DF-1 cells or CEFs per well) and $TCID_{50}$ was analyzed with Spearman-Karber fomula. For infection assays, DF-1 cells or CEFs were seeded at a density of 5×10^5 cells per well in a 12-well plate. Approximately 5×10^5 $TCID_{50}$ of free ALV-J particles and SE-ALV-J were added to the cells. After 2 h of incubation, the medium was replaced with fresh maintenance medium and incubated at 37 °C with 5% CO_2 for 72 h. At 12, 24, 36, 48, or 72 h post-infection, cell samples were collected, and total RNA were extracted to determine ALV-J RNA copy numbers by using reverse transcription-quantitative RT-qPCR. At the same time, the collected cell samples were lysated and subjected to analyze ALV-J gp85 protein expression by Western blotting.

2.9. Western blotting

Cells and SE were lysed in RIPA lysis buffer (Santa Cruz Biotechnology, Inc.,USA), loaded on a 10% SDS gel, resolved using SDS-PAGE and transferred to PVDF membranes (EMD Millipore). Membranes were blocked in 5% skimmed milk, 0.05% Tween 20 in PBS, and subsequently incubated with the primary antibodies at 4 °C overnight, followed by incubation with horseradish peroxidase-conjugated secondary antibodies against goat anti-rabbit IgG or goat anti-mouse IgG (Beyotime Institute of Biotechnology, China) at room temperature for 1 h. Signals were visualized using an ECL Advance western blotting detection kit (CW Biotechnology, China). Bands were imaged using an Azure c300 digital imager system (Azure Biosystems), CD81 (System Biosciences, Inc., USA), CD63 (System Biosciences, Inc., USA), tumor susceptibility gene 101 (TSG101; Absin Biotechnology, China), GPR78 (Abcam, UK), β-actin (CW Biotechnology, China), and ALV-J p27, gp37 and gp85 (made in our laboratory) were used primary antibodies.

2.10. Analysis and quantification of ALV-J RNA

To detect ALV-J RNA, total RNA was extracted from seminal EVs (RNase treated) using TRIzol® reagent (Thermo Fisher Scientific, Inc., USA) and reverse transcribed into cDNA using a Prime-Script™ cDNA synthesis kit (Takara Bio, Inc., China). The full-length ALV-J genome was divided into three overlapping fragments (A, B and C) to be amplified, and the primers for each fragment are prensent in Supplementary Table S1. For quantification of the RNA copies of ALV-J in ALV-J-infected or SE-ALV-J treated cells, total RNAs were isolated from cultured cells and reverse transcribed into cDNA as described above. RT-qPCR was performed using a CFX96 system (Bio-Rad Laboratories, Inc, USA) using Power SYBR Green PCR Master Mix (Roche Diagnostic) according to the manufacturer's protocol. To construct a standard plasmid, a 148 bp fragment of ALV-J *gp85* gene was amplified with the primer pairs J-F and J-R (Supplementary Table S1), and then cloned into the pMD-19T vector (Takara Bio, Inc., China). The copy number of viral RNA was calculated based on the results for the standard plasmid diluted 10-fold (1×10^1 copies/μL to 1×10^9 copies/μL). Each sample was analyzed in triplicate. For analysis of the homology of ALV-J, total RNAs were extracted form ALV-J strain GD1109, SE-ALV-J, and ALV-J isolated from the progeny chicks, and reverse transcribed into cDNA as described above. The gp85 coding sequence (924 bp) was amplified using the primer pair gp85-F and gp85-R (Supplementary Table S1) with the FOD-FX (Toyobo Life Science, China). The purified RT-PCR products were cloned into the pMD-19T vector for sequencing. Sequence alignment was performed using Lasergene version 7.1 (DNAStar, Inc.)

2.11. Transmission of ALV-J infection via SE-ALV-J

A total of 18 SPF hens were randomly selected from 24 weeks old laying SPF hens that were prepared in advance as described above and divided into 3 groups, with 6 SPF laying hens per group. Semen samples were collected from 5 healthy roosters with no ALV-J infection and

mixed with SE or free ALV-J for artificial insemination of different groups of SPF hens. For detection of infection and transmission of ALV-J mediated by SE-ALV-J, 3 groups of artificial insemination experiments were performed. Group A hens were artificially inseminated with 40 μL of semen from healthy roosters mixed with 40 μL of SE-Mock and used as the mock control. Group B and C hens were artificially inseminated with 40 μL of semen from healthy roosters mixed with equal viral titers (0.5 × 10^5 TCID$_{50}$) of SE-ALV-J and free ALV-J, respectively. Whole blood samples from all the hens in all 3 groups were collected at 1, 2, 3, and 4 week post-insemination. Blood plasma prepared from each individual hen was inoculated into DF-1 cells for ALV-J isolation as previously described (Wang et al., 2020), and the serum samples were assessed for the presence of ALV-J antibody using ELISA detection kits (IDEXX Laboratories). The eggs were collected from the different groups of SPF hens and tested for p27 antigen in egg albumin with an Avian Leukosis Virus Antigen Test Kit (IDEXX Laboratories, USA). Fertilized eggs from the 3 different groups of SPF hens were collected for hatching. Whole blood samples of hatched progeny chicks from the 3 different groups of SPF hens were collected at an age of 1 day, as well as at subsequent 1–3 weeks of age, and assessed for ALV-J infection status through viral isolation as described above. Meconiums were sampled from hatched progeny chicks

and tested for p27 antigen using a direct p27 ELISA kit. All samples collected were analyzed in duplicate.

2.12. Statistical analysis

Statistical analysis was perfomed using GraphPad Prism version 7.0 (GraphPad Software, Inc.). Results are presented as the mean ± standard error of the mean. Differences were compared using an unpaired Student's *t*-test. $P < 0.05$ was considered to indicate a statistically significant difference.

3. Results

3.1. Isolation and characterization of SE from ALV-J-infected rooster semen

To ensure the purity of the SE-ALV-J, we optimized a two-step isolation method to extract and purify SE from ALV-J-infected rooster semen by using Exo-Quick-TC™ in combination with CD63-immunomagnetic beads affinity purification. After Exo-Quick centrifugation, the free ALV-J particles (Free ALV-J) were present in the
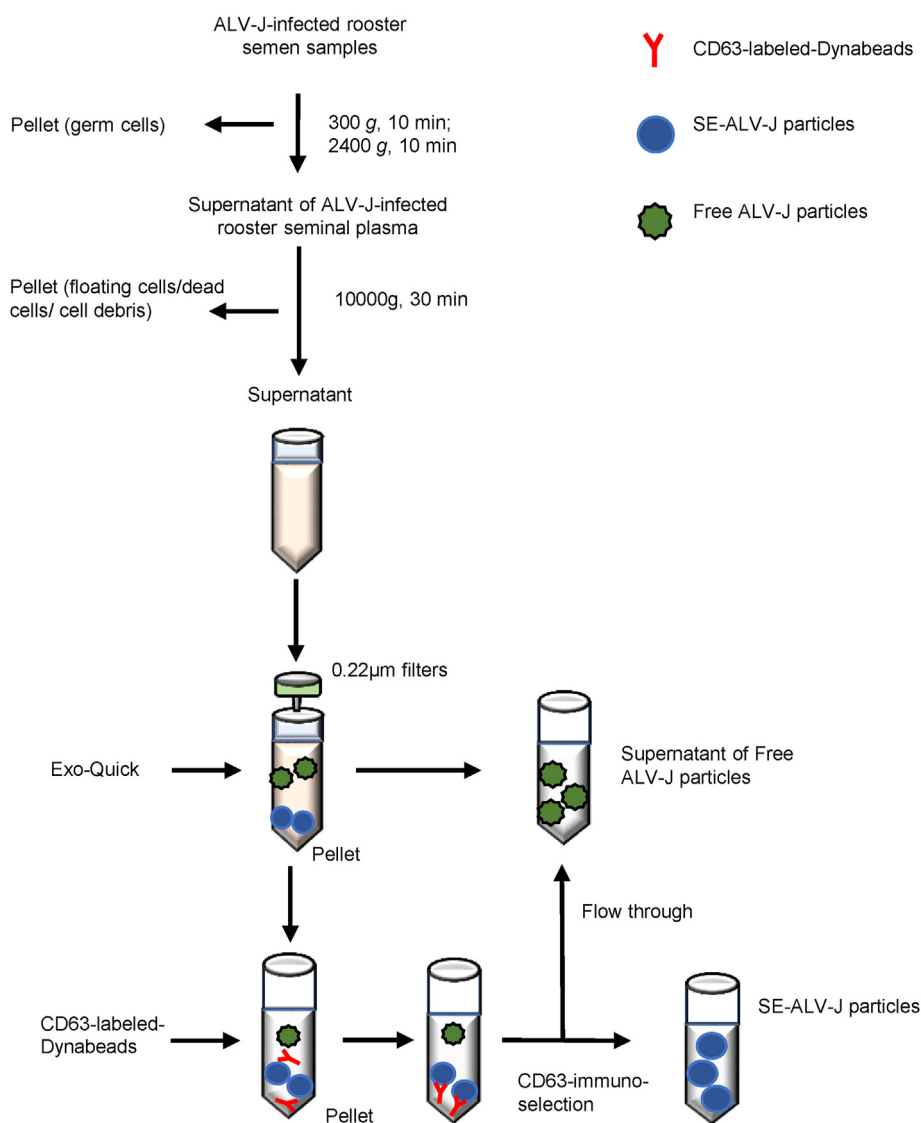

Fig. 1. Schematic presentation of Exo-Quick + CD63 immuno-magnetic selection for SE-ALV-J purification. SE-ALV-Js were separated from free ALV-J particles by binding to CD63 immuno-magnetic beads, and then purified SE-ALV-Js were eluted from Dyna-beads.

supernatant and flow through following CD63 immuno-magnetic isolation (Fig. 1). The morphology of the isolated SE-ALV-J was verified by using transmission electron microscopy (TEM) examination and nanoparticle tracking analysis (NTA). TEM showed that the purified SE-ALV-J exhibit a classical cup-shaped appearance with a lipid bilayer membrane, while the purified ALV-J particles display a spherical appearance with an enveloped structure (Fig. 2A). The results of NTA showed that the size distribution patterns were similar between SE-ALV-J and SE-Mock, over 85% and 80% of SE were observed with sizes ranging from 50 to 200 nm, respectively (Fig. 2B). Next, the purified SEs were characterized through an analysis of EV-specific

markers by Western blotting. Both SE-Mock and SE-ALV-J expressed the marker proteins CD81, CD63, and tumor susceptibility gene 101 (TSG101) but lack of expression of GRP78 (endoplasmic reticulum marker) (Fig. 2C), suggesting that there was no contamination with endoplasmic vesicles in the purified SE. Subsequently, the purified SE-ALV-J was further characterized by immunogold labeling with antibodies against the marker CD63 and ALV-J envelope protein gp85. The results showed that the CD63 marker protein but not the viral gp85 protein could be probed in the SE-ALV-J (Fig. 2D). Collectively, these results showed that there was no cellular and free ALV-J particles contamination in the purified SE-ALV-J.
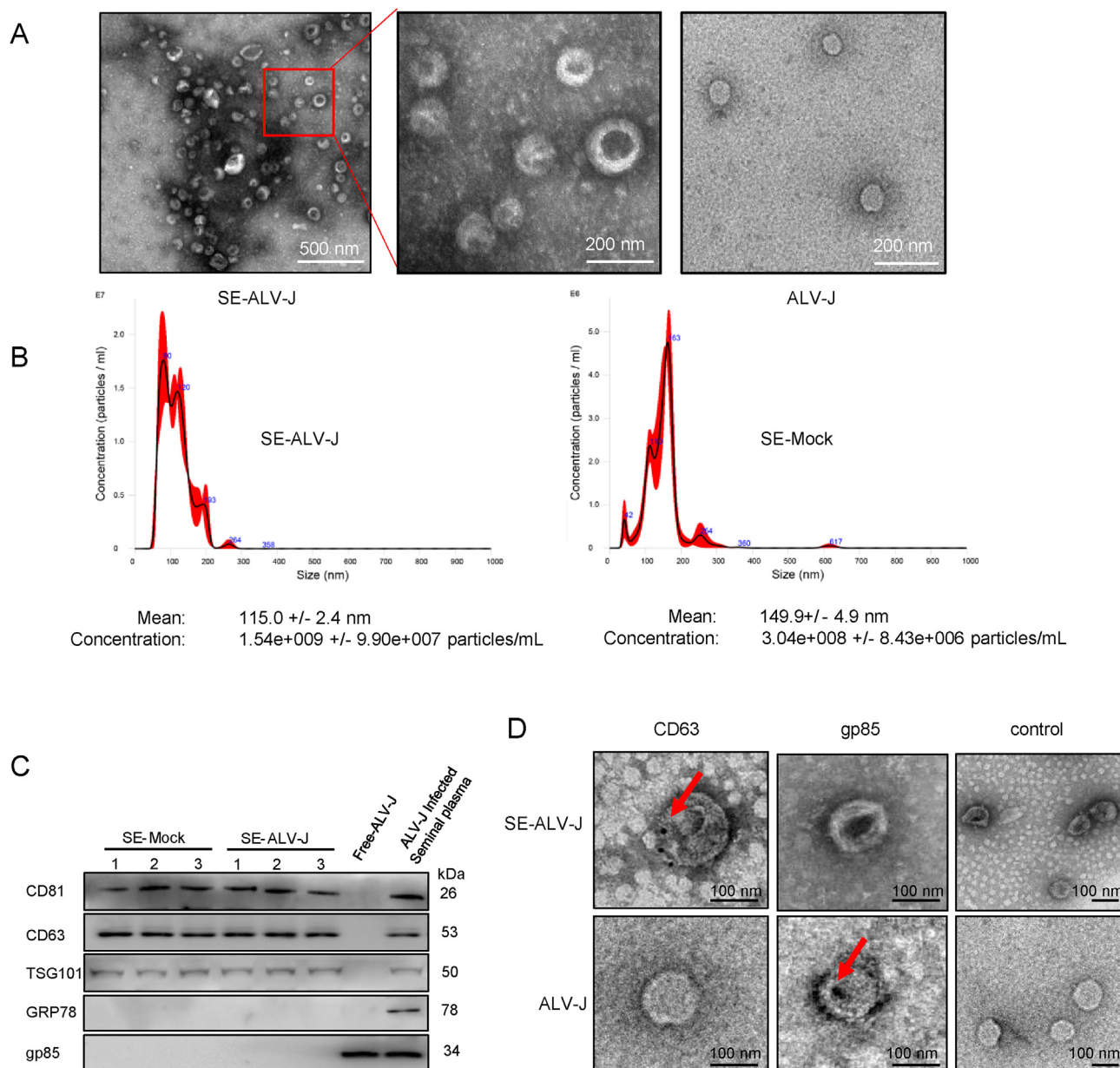

Fig. 2. Isolation and characterization of SE from ALV-J-infected rooster seminal plasma. **A** Transmission electron microscopy observations of negatively stained SE derived from ALV-J-infected rooster semen (SE-ALV-J) and purified virions (free ALV-J). Representative images of purified SE-ALV-J and ALV-J are shown. **B** Size distribution and concentration of SE-ALV-J and SE-Mock were determined by NTA. Results are represented as the average distribution of three independent isolations of SE-ALV-J and SE-Mock. **C** Western blot analysis on SE derived from three different mock- or ALV-J-infected rooster seminal plasmas samples using antibodies against the common exosome markers CD81, CD63 and TSG101, and the endoplasmic reticulum marker GRP78. Purified virions and ALV-J-infected rooster seminal plasma were used as the controls. **D** Immunoelectron microscopy of purified SE-ALV-J or virions from ALV-J infected rooster seminal plasma. Immunogold labeling was performed using antibodies against exosome marker protein CD63 and viral protein gp85. The antibody staining with gold particles is indicated by arrows. One representative experiment of three is shown.

3.2. SE derived from ALV-J-infected rooster semen contained ALV-J components

In order to characterize the contents of SE purified from ALV-J-infected rooster seminal plasmas, we performed RNA sequencing on pooled SE-ALV-J and pooled SE-Mock. A total of 43,074,934 and 22,983,798 reads was identified for SE-ALV-J and SE-Mock, respectively. These reads were then mapped to the chicken reference genome (gal-Gal6) using Bowtie2 version 2.1.0 (Langmead and Salzberg, 2012). As shown in supplementary Table S2, the percentage of mapped reads was 54.13% and 40.39% for SE-ALV-J and SE-Mock, respectively, indicating that both SE-ALV-J and SE-Mock are derived from the cells of the chickens. The reads were further mapped to the ALV-J strain GD1109 genomic RNA sequences, as well as its *Gag*, *Pol* and *Env* coding region sequence (CDS) of ALV-J strain GD1109. The total mapped reads and fractions to GD1109 genomic RNA, mapped reads and percentages to *Gag*, *Pol* and *Env* CDS are listed in supplementary Table S3. The percentages of the total mapped reads of SE-ALV-J and SE-Mock to ALV-J strain GD1109 genomic RNA sequences were 22.59% and 0.45%, respectively. Furthermore, the mapped reads of SE-ALV-J to Gag, Pol and Env CDS were much higher than the mapped reads of SE-Mock (supplementary Table S3). To further validate whether ALV-J RNAs were present in SE-ALV-J, we designed RT-PCR primers to amplify the entire genomic RNA of ALV-J in three overlapping fragments (A, B, and C) as depicted in Fig. 3 (top chart). As shown in Fig. 3 (bottom gel image), all three overlapped fragments were amplified successfully from SE-ALV-J, which indicated that SE-ALV-J contained the complete ALV-J RNA genome. Taking together, the above data demonstrated that SE-ALV-J contained ALV-J genomic RNA.

3.3. SE-ALV-J can transfer ALV-J components to uninfected naive cells

Giving that ALV-J components were present in the purified SE-ALV-J, it prompted us to investigate if SE-ALV-J can transfer ALV-J components to uninfected naive cells. To this end, DiO-labeled DF-1 cells were incubated with DiI-labeled SE-ALV-J and DiI-labeled SE-Mock, respectively, and confocal fluorescence microscopy was employed to visualize the contour of the cells. As shown in Fig. 4A, both SE-ALV-J and SE-Mock were observed being colocalized with the plasma membrane, which

signified that both SE-ALV-J and SE-Mock were uptaken by the DF-1 cells. Notably, Alexa Fluor-594 labeled viral protein gp85 was detected in the cytoplasm of DF-1 cells exposed to SE-ALV-J, but not detected in the cytoplasm of DF-1 cells co-incubated with SE-Mock (Fig. 4B). Furthermore, Alexa Fluor-488 dye labeled viral protein gp85 was co-localized with SE-ALV-J within the cytoplasm of DF-1 cells, as shown in Fig. 4C, indicating that SE-ALV-J contains ALV-J envelope protein gp85. Moreover, much more SE-ALV-J were uptaken by DF-1 cells after incubation between DiO-labeled DF-1 cells and DiI-labeled SE-ALV-J for 4 h than that of 2 h, as indicated by confocal fluorescence microscopy, as shown in Fig. 4D, confirming that the uptake of SE-ALV-J by DF-1 cells was an active process. This experimental evidence indicated that SE-ALV-J could be taken up by DF-1 cells and subsequently transferred ALV-J components to the DF-1 cells.

3.4. SE-ALV-J transmits ALV-J and establishes productive infection in host cells

Since the purified SE-ALV-J can carry and deliver ALV-J components into recipient cells, it prompted us to further understand whether SE-ALV-J can transmit ALV-J infection to uninfected naive cells. For this purpose, the purified SE-ALV-J was incubated with DF-1 cells and primary chicken embryo fibroblasts (CEFs), respectively, and $TCID_{50}$ assays were performed to determine the viral titers in the SE-ALV-J-treated DF-1 cells and CEFs. Cells infected with free ALV-J were used as the positive control. As shown by the results in Fig. 5A, the purified SE-ALV-J generated high viral titers in both DF-1 cells and CEFs, which were similar to the levels determined in cells infected with free ALV-J. To further characterize SE-ALV-J *in vitro*, DF-1 cells were incubated with the purified SE-ALV-J, and real-time qPCR (RT-qPCR) designed for detection of viral RNA contents and Western blotting for viral gp85 protein expression levels were performed at 12, 24, 36, 48, and 72 h post treatment. Cells infected with free ALV-J with equal viral titers were used as the positive control, while cells incubated with SE-Mock were used as the negative control. As shown in Fig. 5B, RT-qPCR data indicated that the levels of viral RNA in SE-ALV-J treated cells showed a continuous increment trend over the time points, but replicating slower than the free ALV-J. At the same time, the results of Western blotting showed that the expression levels of gp85 protein between the SE-ALV-J and free ALV-J
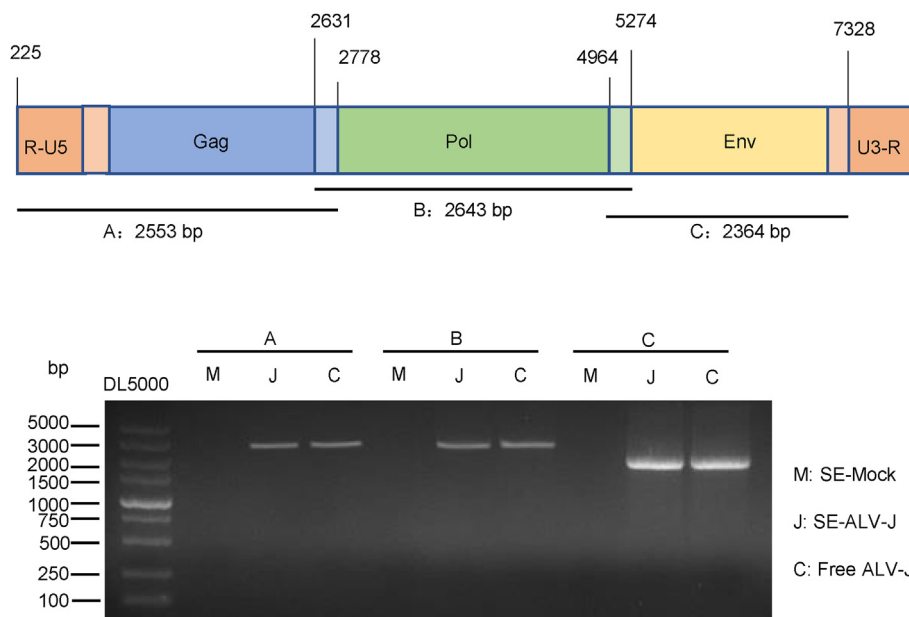

Fig. 3. Components of SE derived from ALV-J-infected rooster seminal plasma. ALV-J genomic RNA in SE-ALV-J was detected using reverse transcription-PCR. Three overlapping fragments (**A, B**, and **C**) were designed based on the genome sequence of the ALV-J strain GD1109. SE-Mock and purified free ALV-J particles were used as the controls.
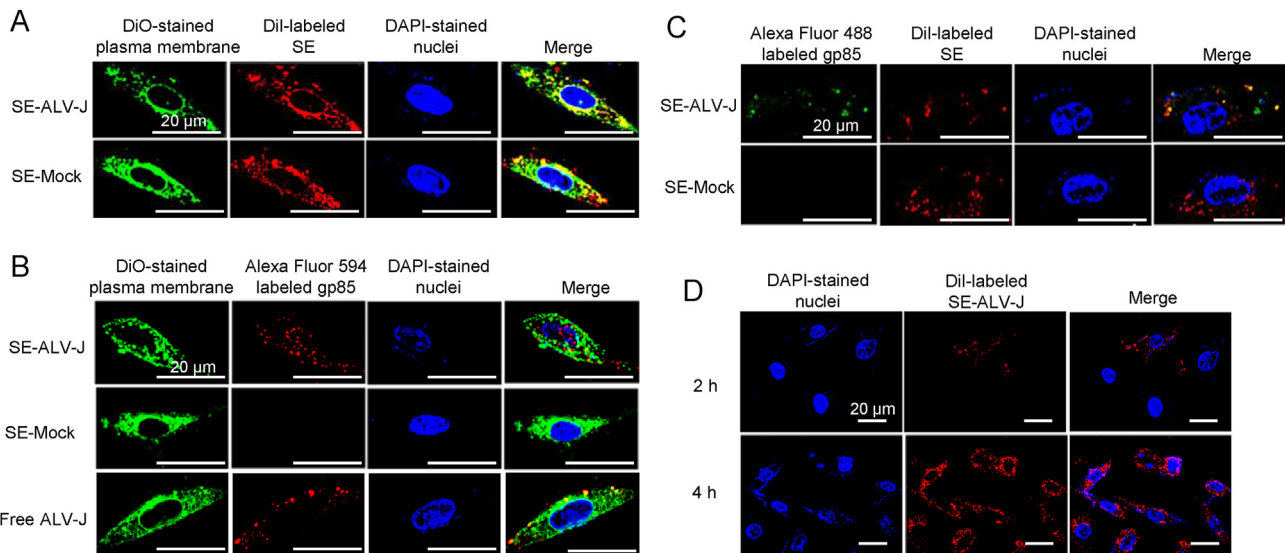
Fig. 4. SE-ALV-J can transmit ALV-J components to DF-1 cells. **A** Both SE-ALV-J and SE-Mock can be uptaken into DF-1 cells. Purified SE-ALV-J or SE-Mock were firstly stained with the red fluorescent dye DiI for 20 min, and then were added to DF-1 cells. After 2 h of incubation at 37 °C, the cells were fixed and stained with the green fluorescent dye DiO. The cell nuclei were stained with DAPI (blue) and observed under a confocal microscopy. Scale bar, 20 μm. (**B, C**) SE-ALV-J contained ALV-J envelope protein gp85. After being incubated with purified SE-ALV-J or SE-Mock for 2 h, DF-1 cells were incubated with an anti-gp85 antibody and then stained with Alexa Fluor 594-conjugated anti-mouse IgG (red) or Alexa Fluor 488-conjugated anti-mouse IgG (green). Confocal co-localization analysis of SE-ALV-J or SE-Mock and viral protein gp85 were performed. The cell nuclei were stained with DAPI (blue). Scale bar, 20 μm. **D** The confocal image shows the co-localization of DiO-labeled DF-1 cells incubated with DiI-labeled SE-ALV-J (red) for 2 h and 4 h, respectively. The cell nuclei were stained with DAPI (blue). Scale bar, 20 μm.

groups at all tested time points remained consistent (Fig. 5D and E). As expected, ALV-J viral RNA and viral protein gp85 were not detected in the cells treated with SE-Mock (Fig. 5B–E). These experimental data confirmed that a productive infection was established in DF-1 cells inoculated with SE-ALV-J. Furthermore, it was shown that ALV-J RNA and viral protein gp85 were clearly detectable in the lysates of CEFs co-cultured with SE-ALV-J by Real-time qPCR and Western blot, respectively (Fig. 5C and E), confirming a similar productive infection was established in CEFs after treatment with SE-ALV-J. The expression of the ALV-J viral proteins p27, gp85, and gp37 can also be detected by Western blotting in DF-1 cells and CEFs treated with SE-ALV-J (Fig. 5F), further confirming the establishment of productive infections. These observations taken together suggested that SE-ALV-J had the same efficiency as free ALV-J in infection of naive cells and could establish productive infections in host cells.

3.5. Vertical transmission of ALV-J infection can be mediated by SE-ALV-J in vivo

Given that SE-ALV-J are capable of transmitting infection and establishing productive infection *in vitro*, which prompted a question on SE-ALV-J mediating infection of ALV-J *in vivo*. First, whether SE-ALV-J could transmit infection of ALV-J to specific pathogen-free (SPF) hens through a series of artificial insemination was determined. SPF hens were artificially inseminated with healthy roosters' semen mixed with SE-Mock (Group A, used as a mock control group). SPF hens were artificially inseminated with healthy roosters' semen mixed with equal viral titers of SE-ALV-J (group B) or free ALV-J (group C). ALV-J infection status of the SPF hens in all three groups was subjected to test for the presence of virus and ALV-J antibody in blood plasma and serum individually at 1-, 2-, 3-, and 4-week post insemination. The control group hens at 1–4 weeks post insemination were all tested negative for virus and antibody response. However, all group B hens at 1–4 weeks post insemination were positive both on virus and antibody response. The group C hens at 1–4 weeks post insemination were also tested negative for ALV-J and ALV-J antibody response (Table 1). Furthermore, eggs were collected for 4 weeks after artificial insemination from the hens in

groups A, B and C to determine the vertical infection of ALV-J using an ALV p27 ELISA kit. All 23 eggs collected from the control group hens and 20 eggs from hens in group C were negative for p27 antigen. In contrast, the p27 antigen was present in egg albumin of all 25 eggs collected from the hens in group B (Table 2). These results suggest that the infection of SPF hens by ALV-J can be mediated via SE-ALV-J and the infected hens shed ALV-J antigens into their egg albumin.

To further investigate whether SE-ALV-J was capable of transmitting infection of ALV-J from hen to progeny, the eggs were also collected from group A, B and C SPF hens and tested for presence of p27 antigen in meconium as well as for virus to hatch chicks. Consistent with the results in egg albumin, p27 antigens were detected in meconium samples of all 1-day-old chicks of the group B hens, while none of chicks hatched from the group A and C hens was positive for p27 antigen (Table 1). Furthermore, ALV-J was isolated from all 16 chicks of the group B hens at one-day-old of age up to three weeks of age, while no virus viremia was detected in any of chicks of the group A and C hens (Table 1). Subsequently, we compared the homology of ALV-J *gp85* gene nucleotide sequences isolated from the group B progeny chicks, SE-ALV-J and original GD1109 challenge virus. As shown in Table 3, *gp85* gene of the ALV-J isolated from the group B progeny chicks exhibited a 99.1%–99.5% and a 98.9%–99.3% nucleotide sequence identity with the ALV-J isolated from five SE-ALV-J samples and the original GD1109 ALV-J strain of viruses, respectively. Furthermore, the gp85 of ALV-J isolated from five SE-ALV-J samples shared 98.8%–99.4% nucleotide sequence identity with the original challenge virus GD1109. These data provided key evidence that the ALV-J isolated from the group B progeny chicks came from the original challenge virus, whilst further supporting the notion that SE-ALV-J but not ALV-J variation mediates vertical transmission of ALV-J infection from hen to progeny.

4. Discussion

Extracellular vesicles were initially hypothesized to serve as vehicles to discard cellular waste (Muller, 2020), however, they have then been emerged as vital mediators of cell-to-cell communication by shuttling biologically active proteins, lipids and RNAs between cells, which serving
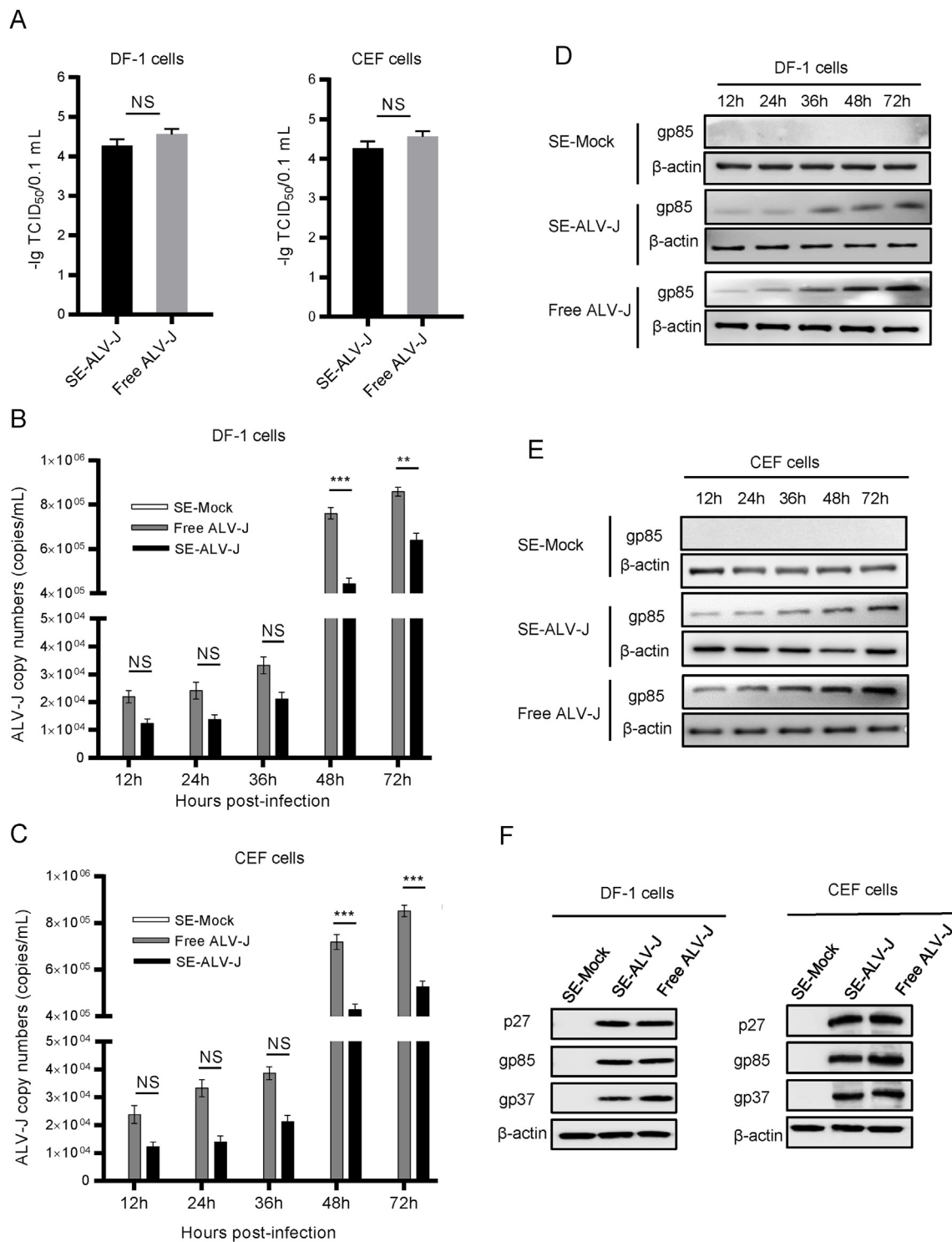
Fig. 5. SE-ALV-J transmits ALV-J and establishes productive infections in host cells. A DF-1 cells and CEFs were treated with purified SE-ALV-J or infected with ALV-J, respectively, and the viral titers were determined with TCID50 assay. (**B** to **E**) Real-time qPCR and western blot analysis demonstrated productive infection of DF-1 cells and CEFs after treatment with SE-ALV-J. DF-1 cells and CEFs were cocultured with purified SE-ALV-J or infected with free ALV-J at an approximate MOI of 1.0. At 12, 24, 36, 48, and 72 h post treatment or infection, total RNA from DF-1 cells(B) and CEFs (**C**) was extracted and RT-qPCR was performed for detection of viral RNA contents, cell lysates from DF-1 cells (**D**) and CEFs (**E**) were collected and subjected to Western blot test with the antibody against ALV-J gp85 protein. **F** Western blot analysis of ALV-J p27, gp85 and gp37 protein expression in DF-1 cells and CEFs treated with purified SE-ALV-J or infected with free ALV-J for 72 h.

an important role in an array of key pathophysiological processes in literature (Johnstone et al., 1987; Colombo et al., 2014). EVs have also been hypothesized to serve as crucial constituents involved in the pathogenesis of viral infection and serve an important role in life cycle of viruses (Alenquer and Amorim, 2015; Gurunathan et al., 2019). Indeed,

numerous studies have shown that EVs derived from virally-infected cells or bodily fluids are responsible for transmission of viral information, and the cargos of EVs may be involved in both viral infection and transmission (Urbanelli et al., 2019). In the present study, it was shown that SE-ALV-J contains viral RNAs and viral proteins, which can be

Table 1

The viremia results of meconium test of one-day-old chicks and virus isolation results of chicks of the group A-C hens at one-day up to three weeks of age.

Day/week post-hatch	Group[a]	Virus isolation	Meconium
1 day	A	0/13[b]	0/13
	B	16/16	16/16
	C	0/18	0/18
1 week	A	0/13	/
	B	16/16	/
	C	0/18	/
2 week	A	0/13	/
	B	16/16	/
	C	0/18	/
3 week	A	0/13	/
	B	16/16	/
	C	0/18	/

[a] Group A = SPF hens were artificially inseminated with 40 μL healthy roosters' semen mixed with 40 μL SE-Mock; Group B and C = SPF hens were artificially inseminated with 40 μL healthy roosters' semen mixed with equal viral titers $(0.5 \times 10^5$ TCID$_{50}$) of SE-ALV-J and free ALV-J, respectively.

[b] No.of positive samples/total no. of samples.

Table 2

The infection status of SPF hens and eggs post artificial insemination with different pre-treated semen.

Week post-insemination	Group[a]	Virus isolation	ALV-J antibody response	p27 antigen of eggs
1 week	A	0/6[b]	0/6	0/23[c]
	B	6/6	6/6	25/25
	C	0/6	0/6	0/20
2 week	A	0/6	0/6	
	B	6/6	6/6	
	C	0/6	0/6	
3 week	A	0/6	0/6	
	B	6/6	6/6	
	C	0/6	0/6	
4 week	A	0/6	0/6	
	B	6/6	6/6	
	C	0/6	0/6	

[a] Group A = SPF hens were artificially inseminated with 40 μL healthy roosters' semen mixed with 40 μL SE-Mock; Group B and C = SPF hens were artificially inseminated with 40 μL healthy roosters' semen mixed with equal viral titers $(0.5 \times 10^5$ TCID50) of SE-ALV-J and free ALV-J, respectively.

[b] No. of positive hens/total no. of hens.

[c] No. of positive eggs/total no. of eggs.

Table 3

ALV-J gp85 gene nucleotide sequence identity comparisons among ALV-J isolates of the progeny chicks of the SE-ALV-J pretreated SPF hens, the SE-ALV-J, and the original GD1109 challenging virus.

	GD1109[a]	SE-ALV-J	progeny chicks
GD1109	–	98.8%–99.4%	98.9%–99.3%
SE-ALV-J	98.8%–99.4%	–	99.1%–99.5%
progeny chicks	98.9%–99.3%	99.1%–99.5%	–

[a] GD1109 = original challenging virus.

transmitted to naive cells and establish a productive infection. Our data also demonstrated that SE-ALV-J is capable of mediating vertical transmission of ALV-J from hen to progeny.

As ALV-J virions and SE share significant similarities including size, buoyancy densities and sedimentation velocities, conventional sucrose gradient differential ultracentrifugation cannot efficiently extract SE-ALV-J free of cellular and viral contamination. In order to overcome these limitations, a CD63 immunomagnetic bead isolation method was optimized to further purify SE-ALV-J isolated from ALV-J-infected rooster semen. This two-step purification method appeared more stringent and ensured the SE-ALV-J separation without carryover of free viruses, thereby

further underscoring the capacity of SE-ALV-J to transmit ALV-J infection (Zhou et al., 2020). TEM analysis showed that both SE-ALV-J and SE-Mock displayed the classical morphological characteristics of EVs (Fig. 2A), which confirmed the purity of SE-ALV-J and SE-Mock. NTA showed that SE contained majority of the EVs size ranging from 50 to 200 nm (Fig. 2B), which suggested the feasibility of the isolation methods in obtaining the highly pure SE-ALV-J and SE-Mock. Although the size distribution of SE particles between SE-ALV-J and SE-Mock is different, they both resembled to that described in previous studies (Colombo et al., 2014; van Niel et al., 2018). Since retrovirus and exosomes share the same secretion pathway (Thery et al., 2002), the reason why SE-Mock is larger than SE-ALV-J is probably that SE-Mock is mostly composed of microvesicles (~100–1000 nm), but SE-ALV-J is mostly exosomes (<150 nm). Exosomes and microvesicles both are one of the three major types of extracellular vesicles, which have been studied and discussed by a number of groups. The purified SE-Mock and SE-ALV-J also expressed the EV-marker proteins CD81, CD63 and TSG101, and did not express the endoplasmic reticulum marker protein GRP78 (Fig. 2C), which suggesting that both SE-ALV-J and SE-Mock came from non-endoplasmic reticulum sources. Immune-electron microscopy analysis confirmed that there were no free ALV-J virions in the purified SE-ALV-J (Fig. 2D). These results suggest that both the purified SE-ALV-J and SE-Mock were free of viral and no cellular contamination.

Recent studies have shown that the constituents of EVs can be altered following viral infection (Crenshaw et al., 2018)(49). The results of the present study showed the enrichment of ALV-J viral RNAs in the purified SE-ALV-J, including the complete ALV-J genomic RNA (Fig. 3). In addition to packaging viral genomes, EVs can also incorporate a set of viral-encoded proteins that promote viral spread. Indeed, three structural proteins, p27, gp37 and gp85, were identified in the purified SE-ALV-J using Western blotting (Fig. 5F). These results demonstrated that the contents of SE-ALV-J were altered compared with SE-Mock, and the contents of SE-ALV-J reflected the pathological state of the host cells. Upon exposure to DF-1 cells, both SE-ALV-J and SE-Mock were uptaken by DF-1 cells (Fig. 4A). Furthermore, the intact SE-ALV-J taken up by DF-1 cells was capable of transferring ALV-J components to non-infected cells (Fig. 4B and C). Based on our findings, we speculate that if viral components were packaged into EVs, they were exported and subsequently transmitted to the neighboring cells, thereby regulating host cellular behavior and producing productive infections. In recent years, increasing evidence suggested that EVs derived from virally infected cells or bodily fluids can carry and deliver viral genomes, mRNAs, microRNAs, proteins, and/or even virions into recipient cells, thereby facilitating viral infection and transmission, as shown for PRRSV, HCV and many other animal viruses (Madison et al., 2014; Longatti, 2015; Vora et al., 2018; T Wang et al., 2018; Zhou et al., 2018; Sadri et al., 2019; Slonchak et al., 2019). For example, PRRSV-infected cell derived-exosomes contain viral genomic RNA and partial viral proteins, which can transfer PRRSV to susceptible and non-susceptible cells and establish a productive infection (T Wang et al., 2018). Exosomes released from HCV-infected cells containing infectious viral RNA and proteins were also shown capable of mediating HCV transmission between hepatocyte-like cells (Bukong et al., 2014). In the present study, SE-ALV-J transmitted ALV-J RNA and viral protein to uninfected naive cells and functioned effectively as free ALV-J virus, but exhibited different replication capability within recipient cells. Infection of naive DF-1 and CEFs with infectious SE-ALV-J increased viral RNA content and viral protein levels within the recipient host cells, which confirmed the establishment of productive infections and further suggested an important role for SE-ALV-J as ALV-J viral RNA and protein transporters. These results strongly suggested that ALV-J also took advantage of the seminal exosomal pathway to transfer virus to naive cells and establish a productive infection.

A significant finding of this study is that SPF hens were infected by ALV-J through artificial insemination of semen from healthy roosters mixed with SE-ALV-J, which for the first time revealed that SE-ALV-J is capable of mediating ALV-J infection in SPF hens. Since our data have demonstrated that SE-ALV-J carries and delivers viral RNA and protein

into recipient cells, which subsequently is capable of establishing productive infection *in vitro*, the SE-ALV-J mediating ALV-J infection of SPF hens could be resulted from two plausible events. One would be that ALV-J infection changes the immunosuppressive properties of SE-ALV-J by hijacking the exosomal pathways, thereby allowing SE-ALV-J to promote ALV-J infection and to impair the protective immune response against the infectious virus. The other would be that ALV-J infection triggers alterations in the composition and signal transduction of SE-ALV-J, which may promote a series of functional effects, such as increased target cell activation and cytokine expression, therefore, compromising the protective immune response, and thereby enhancing ALV-J entry into target cells. Another significant finding from the present study is that SE-ALV-J further mediated the infection and transmission of ALV-J from hen to progeny. Although the underlying mechanistic events are heretofore unknown, several plausible explanations might somewhat light up the vertical transmission of ALV-J infection event from hen to progeny via SE-ALV-J. Since the ALV-J viral RNA and viral proteins were present inside of SE-ALV-J, one possible explanation that reconciles these findings is that SE-ALV-J provided a suitable environment for ALV-J viral RNA and viral proteins, thereby it contributed to the protection of these ALV-J-related molecules from enzymatic degradation and transportation of the cargos from ALV-J infected-hen to the progeny through overcoming biological barriers and eluding immune recognition. Another possible explanation is that the SE-ALV-J mediated transmission of ALV-J through endocytic uptake of infectious SE-ALV-J into host cells, which were not restricted by the cellular surface receptors, thus the spread of ALV-J from infected-hen to progeny is very fast and efficient. Notably, SPF hens cannot be infected by ALV-J through artificial insemination of semen from healthy roosters mixed with free ALV-J virus. Therefore, it is possible that SE derived from the semen of healthy roosters would inhibit ALV-J infection and/or potently block viral transmission, thereby limiting disease progression in SPF hens. Consistent with this hypothesis, previous studies have showed that healthy human semen-derived SE can inhibit infection and transmission of HIV-1 *in vitro* (Madison et al. 2014, 2015). Healthy human semen-derived SE inhibits the binding and recruitment of host transcription factors components, such as NF-κB, SP1 and RNA Pol II, to the promoter of HIV-1 and also inhibits the interaction between Tat proteins, explaining the SE-mediated inhibition of HIV-1 infection and transmission (Welch et al., 2018). However, the exact role of SE in HIV-1 transmission is not fully understood yet. Therefore, the results of the present and previous studies demonstrated that SE can influence viral infection and transmission by either facilitating or blocking it, dependent on the nature of the cells releasing the vesicles, the target cells and many other factors packed in the EVs.

5. Conclusions

In summary, the present study for the first time demonstrated that seminal plasma from ALV-J-infected roosters secreted SE, which transmitted ALV-J infection to SPF hens, and subsequently mediated transmission of ALV-J from the SPF hens to the progeny chicks. Our findings of this study provided experimental evidence on semen extracellular vesicles in relation to ALV-J transmission and infection, which shed valuable insights into the importance of semen extracellular vesicles in mediating vertical transmission of ALV-J.

Data availability

The original contributions presented in the study are included in the article/supplementary material, further inquiries can be directed to the corresponding author/s.

Ethics statement

All experimental protocols were approved by the Animal Ethics Committee at the South China Agricultural University (approval ID:

SYXK-2019-0136). All study procedures and animal care activities were conducted in accordance with the national and institutional guidelines for the care and use of laboratory animals.

Author contributions

Liqin Liao: Investigation, Data curation, Formal analysis, Writing - original draft. Weiguo Chen: Funding acquisition, Methodology, Validation, Writing - review & editing. Xiangyu Zhang: Investigation. Huanmin Zhang: Resources, Writing - review & editing. Aijun Li: Funding acquisition. Yiming Yan: Investigation, Validation. Zi Xie: Investigation. Hongxing Li: Funding acquisition. Wencheng Lin: Funding acquisition, Validation, Writing - review &editing. Jingyun Ma: Resources. Xinheng Zhang: Funding acquisition, Resources, Methodology, Writing - review & editing. Qingmei Xie: Funding acquisition, Conceptualization, Methodology.

Conflict of interest

The authors declare that they have no competing interests.

Appendix A. Supplementary data

Supplementary data to this article can be found online at https://doi.org/10.1016/j.virs.2022.01.026.

References

Alenquer, M., Amorim, M.J., 2015. Exosome biogenesis, regulation, and function in viral infection. Viruses 7, 5066–5083.

Bai, J.H.K., Payne, L.N., Skinner, M.A., 1998. Sequence of host-range determinants in the env gene of a full-length, infectious proviral clone of exogenous avian leukosis virus HPRS-103 confirms that it represents a new subgroup (designated J). Avian Dis. 27, S92–S93.

Bukong, T.N., Momen-Heravi, F., Kodys, K., Bala, S., Szabo, G., 2014. Exosomes from hepatitis C infected patients transmit HCV infection and contain replication competent viral RNA in complex with Ago2-miR122-HSP90. PLoS Pathog. 10, e1004424.

Chahar, H.S., Bao, X., Casola, A., 2015. Exosomes and their role in the life cycle and pathogenesis of RNA viruses. Viruses 7, 3204–3225.

Colombo, M., Raposo, G., Thery, C., 2014. Biogenesis, secretion, and intercellular interactions of exosomes and other extracellular vesicles. Annu. Rev. Cell Dev. Biol. 30, 255–289.

Crenshaw, B.J., Gu, L., Sims, B., Matthews, Q.L., 2018. Exosome biogenesis and biological function in response to viral infections. Open Virol. J. 12, 134–148.

Dhama, K., Singh, R., Karthik, K., Chakraborty, S., Tiwari, R., Wani, M.Y., Mohan, J., 2014. Artificial insemination in poultry and possible transmission of infectious pathogens: a review. Asian J. Anim. Vet. Adv. 9, 211–228.

Fadly, A.M., Smith, E.J., 1999. Isolation and some characteristics of a subgroup J-like avian leukosis virus associated with myeloid leukosis in meat-type chickens in the United States. Avian Dis. 43, 391–400.

Federspiel, M.J., Hughes, S.H., 1997. Retroviral gene delivery. Methods Cell Biol. 52, 179–214.

Gurunathan, S., Kang, M.H., Jeyaraj, M., Qasim, M., Kim, J.H., 2019. Review of the isolation, characterization, biological function, and multifarious therapeutic approaches of exosomes. Cells 8.

Johnstone, R.M., Adam, M., Hammond, J.R., Orr, L., Turbide, C., 1987. Vesicle formation during reticulocyte maturation. Association of plasma membrane activities with released vesicles (exosomes). J. Biol. Chem. 262, 9412–9420.

Kalluri, R., LeBleu, V.S., 2020. The biology, function, and biomedical applications of exosomes. Science 367.

Kechin, A., Boyarskikh, U., Kel, A., Filipenko, M., 2017. cutPrimers: a new tool for accurate cutting of primers from reads of targeted next generation sequencing. J. Comput. Biol. 24, 1138–1143.

Kumar, A., Kodidela, S., Tadrous, E., Cory, T.J., Walker, C.M., Smith, A.M., Mukherjee, A., Kumar, S., 2020. Extracellular vesicles in viral replication and pathogenesis and their potential role in therapeutic intervention. Viruses 12.

Landman, W.J., Post, J., Boonstra-Blom, A.G., Buyse, J., Elbers, A.R., Koch, G., 2002. Effect of an in ovo infection with a Dutch avian leukosis virus subgroup J isolate on the growth and immunological performance of SPF broiler chickens. Avian Pathol. 31, 59–72.

Langmead, B., Salzberg, S.L., 2012. Fast gapped-read alignment with Bowtie 2. Nat. Methods 9, 357–359.

Li, T., Yao, X., Li, C., Zhang, J., Xie, Q., Wang, W., Lu, H., Fu, H., Li, L., Xie, J., Shao, H., Gao, W., Qin, A., Ye, J., 2020. Gp37 regulates the pathogenesis of avian leukosis virus subgroup J via its C terminus. J. Virol. 94.

Lin, Y., Xia, J., Zhao, Y., Wang, F.Y., Yu, S.C., Zou, N.L., Wen, X.T., Cao, S.J., Huang, Y., 2013. Reproduction of hemangioma by infection with subgroup J avian leukosis virus: the vertical transmission is more hazardous than the horizontal way. Virol. J. 10.

Longatti, A., 2015. The dual role of exosomes in hepatitis A and C virus transmission and viral immune activation. Viruses 7, 6707–6715.

Madison, M.N., Jones, P.H., Okeoma, C.M., 2015. Exosomes in human semen restrict HIV-1 transmission by vaginal cells and block intravaginal replication of LP-BM5 murine AIDS virus complex. Virology 482, 189–201.

Madison, M.N., Roller, R.J., Okeoma, C.M., 2014. Human semen contains exosomes with potent anti-HIV-1 activity. Retrovirology 11, 102.

Malhotra, S., Justice, J., Lee, N., Li, Y., Zavala, G., Ruano, M., Morgan, R., Beemon, K., 2015. Complete genome sequence of an American avian leukosis virus subgroup J isolate that causes hemangiomas and myeloid leukosis. Genome Announc. 3, e01586-01514.

Meng, F., Li, Q., Zhang, Y., Cui, Z., Chang, S., Zhao, P., 2018a. Isolation and characterization of subgroup J Avian Leukosis virus associated with hemangioma in commercial Hy-Line chickens. Poultry Sci. 97, 2667–2674.

Meng, F., Li, Q., Zhang, Y., Zhang, Z., Tian, S., Cui, Z., Chang, S., Zhao, P., 2018b. Characterization of subgroup J avian Leukosis virus isolated from Chinese indigenous chickens. Virol. J. 15, 33.

Muller, L., 2020. Exosomes: nanodust? HNO 68, 56–59.

Neoplastic Diseases. Diseases of Poultry. https://doi.org/10.1002/9781119421481.ch152013, 513-673.

Payne, L.N., Brown, S.R., Bumstead, N., Howes, K., Frazier, J.A., Thouless, M.E., 1991. A novel subgroup of exogenous avian leukosis virus in chickens. J. Gen. Virol. 72 (Pt 4), 801–807.

Payne, L.N., Gillespie, A.M., Howes, K., 1993. Unsuitability of chicken sera for detection of exogenous ALV by the group-specific antigen ELISA. Vet. Rec. 132, 555–557.

Payne, L.N., Nair, V., 2012. The long view: 40 years of avian leukosis research. Avian Pathol. 41, 11–19.

Rubin, H., Fanshier, L., Cornelius, A., Hughes, W.F., 1962. Tolerance and immunity in chickens after congenital and contact infection with an avian leukosis virus. Virology 17, 143–156.

Sadri, N.J., Bokharaei-Salim, F., Karimzadeh, M., Moghoofei, M., Karampoor, S., Mirzaei, H.R., Tabibzadeh, A., Jafari, A., Ghaderi, A., Asemi, Z., Mirzaei, H., Hamblin, M.R., 2019. MicroRNAs and Exosomes: Key Players in HIV Pathogenesis. HIV Med.

Shen, Y., Cai, L., Wang, Y., Wei, R., He, M., Wang, S., Wang, G., Cheng, Z., 2014. Genetic mutations of avian leukosis virus subgroup J strains extended their host range. J. Gen. Virol. 95, 691–699.

Slonchak, A., Clarke, B., Mackenzie, J., Amarilla, A.A., Setoh, Y.X., Khromykh, A.A., 2019. West Nile virus infection and interferon alpha treatment alter the spectrum and the levels of coding and noncoding host RNAs secreted in extracellular vesicles. BMC Genom. 20, 474.

Smith, E.J., Fadly, A.M., 1994. Male-mediated venereal transmission of endogenous avian leukosis virus. Poultry Sci. 73, 488–494.

Thery, C., Zitvogel, L., Amigorena, S., 2002. Exosomes: composition, biogenesis and function. Nat. Rev. Immunol. 2, 569–579.

Urbanelli, L., Buratta, S., Tancini, B., Sagini, K., Delo, F., Porcellati, S., Emiliani, C., 2019. The role of extracellular vesicles in viral infection and transmission. Vaccines (Basel) vol. 7.

van Niel, G., D'Angelo, G., Raposo, G., 2018. Shedding light on the cell biology of extracellular vesicles. Nat. Rev. Mol. Cell Biol. 19, 213–228.

Venugopal, K., Howes, K., Barron, G.S., Payne, L.N., 1997. Recombinant env-gp85 of HPRS-103 (subgroup J) avian leukosis virus: antigenic characteristics and usefulness as a diagnostic reagent. Avian Dis. 41, 283–288.

Vojtech, L., Woo, S., Hughes, S., Levy, C., Ballweber, L., Sauteraud, R.P., Strobl, J., Westerberg, K., Gottardo, R., Tewari, M., Hladik, F., 2014. Exosomes in human semen carry a distinctive repertoire of small non-coding RNAs with potential regulatory functions. Nucleic Acids Res. 42, 7290–7304.

Vora, A., Zhou, W., Londono-Renteria, B., Woodson, M., Sherman, M.B., Colpitts, T.M., Neelakanta, G., Sultana, H., 2018. Arthropod EVs mediate dengue virus transmission through interaction with a tetraspanin domain containing glycoprotein Tsp29Fb. Proc. Natl. Acad. Sci. U. S. A. 115, E6604–E6613.

Wang, G., Wang, Z., Zhuang, P., Zhao, X., Cheng, Z., 2017. Exosomes carring gag/env of ALV-J possess negative effect on immunocytes. Microb. Pathog. 112, 142–147.

Wang, J., Li, M., Li, H., Lin, L., Shi, M., Gu, Z., Gao, Y., Huang, T., Mo, M., Wei, T., Wei, P., 2020. Full-length cDNA sequence analysis of 85 avian leukosis virus subgroup J strains isolated from chickens in China during the years 1988-2018: coexistence of 2 extremely different clusters that are highly dependent upon either the host genetic background or the geographic location. Poultry Sci. 99, 3469–3480.

Wang, P., Lin, L., Li, H., Yang, Y., Huang, T., Wei, P., 2018. Diversity and evolution analysis of glycoprotein GP85 from avian leukosis virus subgroup J isolates from chickens of different genetic backgrounds during 1989-2016: coexistence of five extremely different clusters. Arch. Virol. 163, 377–389.

Wang, Q., Gao, Y., Wang, Y., Qin, L., Qi, X., Qu, Y., Gao, H., Wang, X., 2012. A 205-nucleotide deletion in the 3′ untranslated region of avian leukosis virus subgroup J, currently emergent in China, contributes to its pathogenicity. J. Virol. 86, 12849.

Wang, T., Fang, L., Zhao, F., Wang, D., Xiao, S., 2018. Exosomes mediate intercellular transmission of porcine reproductive and respiratory syndrome virus. J. Virol. 92.

Welch, J.L., Kaddour, H., Schlievert, P.M., Stapleton, J.T., Okeoma, C.M., 2018. Semen exosomes promote transcriptional silencing of HIV-1 by disrupting NF-kappaB/Sp1/Tat circuitry. J. Virol. 92.

Welch, J.L., Madison, M.N., Margolick, J.B., Galvin, S., Gupta, P., Martinez-Maza, O., Dash, C., Okeoma, C.M., 2017. Effect of prolonged freezing of semen on exosome recovery and biologic activity. Sci. Rep. 7, 45034.

Zhang, X., Yan, Z., Li, X., Lin, W., Dai, Z., Yan, Y., Lu, P., Chen, W., Zhang, H., Chen, F., Ma, J., Xie, Q., 2016. GADD45beta, an anti-tumor gene, inhibits avian leukosis virus subgroup J replication in chickens. Oncotarget 7, 68883–68893.

Zhou, D., Xue, J., Zhang, Y., Wang, G., Feng, Y., Hu, L., Shang, Y., Cheng, Z., 2019. Outbreak of myelocytomatosis caused by mutational avian leukosis virus subgroup J in China, 2018. Transboundary Emerg. Dis. 66, 622–626.

Zhou, W., Woodson, M., Neupane, B., Bai, F., Sherman, M.B., Choi, K.H., Neelakanta, G., Sultana, H., 2018. Exosomes serve as novel modes of tick-borne flavivirus transmission from arthropod to human cells and facilitates dissemination of viral RNA and proteins to the vertebrate neuronal cells. PLoS Pathog. 14, e1006764.

Zhou, Y., McNamara, R.P., Dittmer, D.P., 2020. Purification methods and the presence of RNA in virus particles and extracellular vesicles. Viruses 12.